AIAA/AAS Astrodynamics Specialist Conference and Exhibit
16 - 19 August 2004, Providence, Rhode Island

AIAA 2004-5386

Attitude Determination for NPS Three-Axis Spacecraft Simulator

Jong-Woo Kim* , Roberto Cristi†and Brij N. Agrawal ‡
Naval Postgraduate School, Monterey, CA, CA 93943-5106

This paper presents the attitude determination method for the Bifocal Relay Mirror Spacecraft Simulator. The simulator simulates three-axis motion of a spacecraft and has an optical system emulating a bifocal space telescope. The simulator consists of three control moment gyroscopes, rate gyros, two-axis analog sun sensor, and two inclinometers. The five-foot diameter platform is supported on a spherical air bearing to offer a low-torque environment. This paper demonstrates two attitude determination methods employing the measurements from a two-axis analog IR sensor, two inclinometers, and a triaxial gyroscope. The first method implements the conventional Kalman filter algorithm. The second method uses a nonlinear observer derived from the Lyapunov's direct method. Analytical and experimental results are presented to validate the proposed algorithm.

I. Introduction

The Naval Postgraduate School (NPS) Three-Axis Spacecraft Simulator (TASS), which is shown in Fig. 1, is designed for developing and validating acquisition, tracking, and pointing technologies for Bifocal Relay Mirror Spacecraft (BRMS). The BRMS consists of single axis gimballed receive and transmit telescopes. The telescopes are used to redirect the laser light from the ground (or space) to a distant target which necessitate a tight pointing requirement.[1]

The TASS simulates spacecraft three-axis motion and has an optical system simulating a single space telescope. The five- foot diameter TASS platform is supported on a spherical air bearing to offer a low-torque environment. The simulator consists of three variable speed control moment gyroscopes as actuators, rate gyros for angular rate, two-axis analog sun sensor and two inclinometers for attitude sensors. Detailed description of the TASS hardware is given in Ref. 2.

This paper focuses on the development and validation of the attitude determination algorithm of the TASS using two inclinometers, two-axis IR sensor, and a triaxial rate gyroscope. Although inclinometers cannot be used in a spacecraft, they can still be employed in testbeds to get useful attitude information with good accuracy at low cost. Also, if the light source is not far enough, the effect of transitional motion of the IR sensor during the rotation of the testbed should be taken into account when calibrating the IR sensor.

Quaternion attitude parametrization offers a singularity-free method to represent three-dimensional rotations using four-dimensional unit vectors. But the four elements of the unit quaternion cannot be estimated independently because of the normality constraint.

It is a standard approach to include the gyro bias in the overall kinematics model and to estimate the actual attitude by Extended Kalman Filter (EKF) techniques. The EKF, as an extension of the Kalman Filter (KF) to nonlinear models, works satisfactorily when the linearized model exhibits sufficient accuracy. Since the EKF utilizes a linearization at each step, the nonlinear normality constraint of the quaternions cannot be rigidly enforced within the EKF computational structure. Various methods have been developed to overcome this deficiency and are described in Refs. 3, 4, 5, and 6.

The nominal attitude determination method used for the TASS is a basic six-state attitude estimation filter known as the Multiplicative EKF (MEKF).[4] In the MEKF formulation of the TASS, the Modified Rodrigues Parameters (MRPs) are used as an unconstrained representation of the attitude error with quaternion

*NRC Research Associate, Department of Mechanical and Astronautical Engineering, Address, and AIAA Member.
†Associate Professor, Department of Electrical & Computer Engineering , Address
‡Professor, Department of Mechanical and Astronautical Engineering, Address, and AIAA Associate Fellow.

Figure 1. NPS Three-Axis Spacecraft Simulator (TASS)

representing the reference attitude of the defined attitude error. The main advantage of using MRPs over other three dimensional attitude parameterizations is that it has a singularity at 360°.

In this research, we propose a different approach to estimate the attitude and gyro bias. The proposed method, based on a Lyapunov observer, employs both the quaternion and the MRPs, and it fully exploits the nonlinear structure of the attitude kinematics. Consequently, global convergence is analytically guaranteed, which means that the system can recover from large errors.

In what follows, the sensor models are given, then the MEKF is reviewed. Next, a nonlinear Lyapunov observer is derived. Finally numerical and experimental validation of the proposed algorithm is presented.

II. Sensors Model

For the TASS attitude determination, two inclinometers are mounted orthogonally to each other in the testbed's body **x** and **z** axis as shown in Fig. 2 to measure the direction of the gravity vector. The two-axis IR sensor is placed near the edge of the testbed parallel to the body **x** axis vector. Since the IR sensor is not situated at the center of the rotation point, the effect of the transitional motion of the sensor with respect to the light source may have significant effect on the sensor reading.

In this section, we discuss in detail how we can extract gravity vector with two inclinometers then explain a simple way to compensate the transitional motion of the IR sensor on the sensor reading.

A. Inclinometers

The inclinometers mounted on the TASS use capacitive liquid to measure the tilt angle of the platform with respect to the gravity vector. The measuring range of the sensors is ± 30° with a linear angle output accuracy of 0.2°. The transverse axis sensitivity is about 1% of the angle reading at 30° tilt.[7] Figure 3 shows a diagram of an inclinometer fixed in the testbed that is tilted by $+\theta_{I1}$. The vector $\mathbf{L}_1$ lies along the liquid surface and it is perpendicular to the gravity vector. The right-handed sensor coordinate frame i_1 is defined by $\hat{\mathbf{x}}_{I1}$, $\hat{\mathbf{y}}_{I1}$, and $\hat{\mathbf{z}}_{I1}$. The direction of the vector $\mathbf{L}_1$ can be expressed in the sensor frame I_1 as

$$ {}^{I_1}\mathbf{L} = \begin{bmatrix} 1 & -\tan(\theta_{I1}) & 0 \end{bmatrix}^T \tag{1} $$

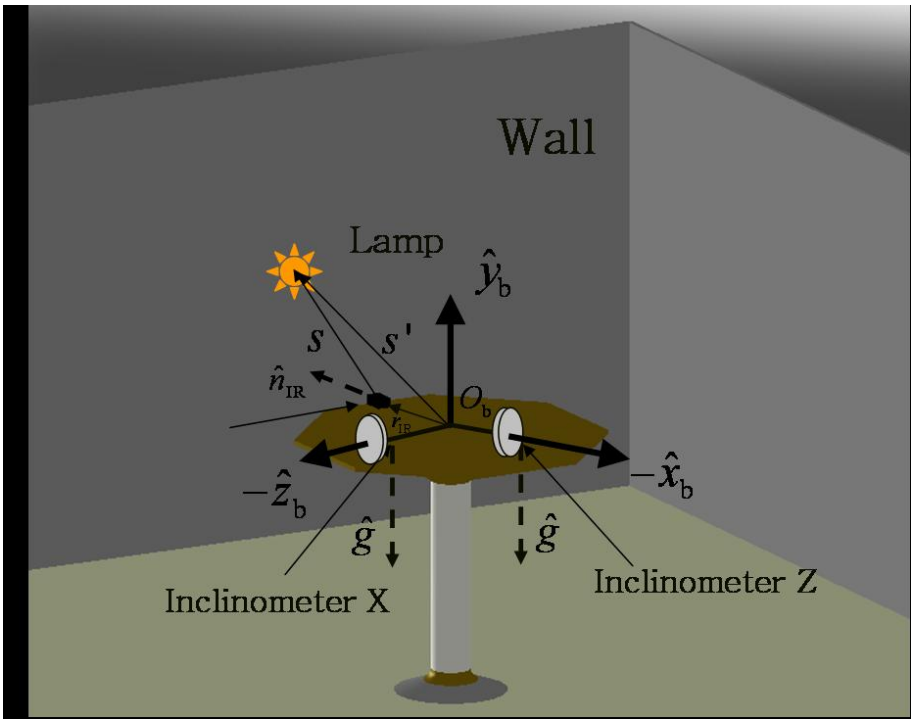

Figure 2. Testbed placement in the NPS lab

with the assumption that its $\hat{\mathbf{x}}_{\mathbf{I1}}$ component equals to one. Using a similar approach for the second inclinometer, the unit gravity vector can be found by taking the cross product between $\mathbf{L}_1$ and $\mathbf{L}_2$ as

$$^B\hat{\mathbf{g}} =^B \mathbf{L}_1 \times^B \mathbf{L}_2/|\mathbf{L}_1 \times \mathbf{L}_2| \tag{2}$$

after converting $\mathbf{L}_1$ and $\mathbf{L}_2$ from the sensor frames (I_1 and I_2) into the testbed's body frame B. With small angle approximations, the $\mathbf{L}_1$ and $\mathbf{L}_2$ output angles correspond to roll and pitch, respectively.

B. IR Sensor

The IR sensor is mounted near the edge of the testbed and senses the 20 W lamp located at 110 cm above the floor and 3 m away from the center (O_b) of the testbed body frame. A top view of the IR sensor and the incident light with the testbed is shown in Figs. 4. From figure 4, we can see that the translational displacement of the IR sensor cannot be neglected since $\mathbf{s}$ and $\mathbf{s}'$ are not parallel with each other. The relation between these two vectors can be expressed as

$$\mathbf{s}' = \mathbf{s} + \mathbf{r}_{IR} \tag{3}$$

where $\mathbf{s}$ is the vector from the sensor to the source light and $\mathbf{r}_{IR}$ is the position vector of the IR sensor. The vector from the testbed center of rotation to the source light is expressed as $\mathbf{s}'$. For the attitude determination, the physical quantity we need as an observation vector is the unity vector of $\mathbf{s}'$ instead of the measured vector $\mathbf{s}$. Equation 3 can be rewritten as

$$\mathbf{s}' = L\hat{\mathbf{s}} + \mathbf{r}_{IR} \tag{4}$$

where L is a scalar representing the magnitude of the vector $\mathbf{s}$ and can be calculated by taking the norm on both sides of Eq. 4 giving

$$|\mathbf{s}'| = |L\hat{\mathbf{s}} + \mathbf{r}_{IR}| \tag{5}$$

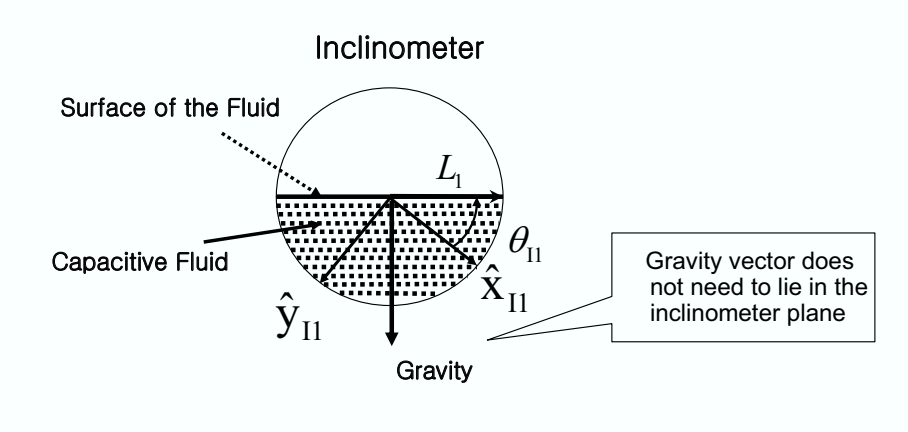

Figure 3. Inclinometer single-axis view

where the quantities $\hat{\mathbf{s}}$, $\mathbf{r_{IR}}$ and $|\hat{\mathbf{s}}'|$ are known. Then letting the known measured vector $\hat{\mathbf{s}} = [x,\ y,\ z]^T$ and the position of the IR sensor $\mathbf{r}_{IR} = [a,\ b,\ c]^T$, the unknown magnitude L can be solved as

$$L = -\frac{zc + yb + xa - \sqrt{2zcyb + 2zcxa + 2ybxa + z^2(-b^2 - a^2 + d^2) + y^2(-c^2 - a^2 + d^2) + x^2(-c^2 - b^2 + d^2)}}{z^2 + y^2 + x^2} \tag{6}$$

Therefore the unit vector $\hat{\mathbf{s}}'$ can be calculated using Eqs. 5 and 6.

III. Attitude Estimation Using Extended Kalman Filter

A widely used six-state attitude estimation method known as the MEKF[4] is implemented for the attitude determination of the TASS. In the MEKF of the TASS, Modified Rodrigues Parameters (MRPs) are used as an unconstrained representation of the attitude error, with some quaternion representing the reference attitude of the defined attitude error. The state vector of the MEKF consists of six elements, three for the MRPs and three for the gyro bias.

A quaternion is defined as

$$\mathbf{q}(t) \equiv \begin{bmatrix} \mathbf{q}_{13}(t) \\ q_4(t) \end{bmatrix} \tag{7}$$

where the vector $\mathbf{q}_{13}$ is

$$\mathbf{q}_{13}(t) \equiv \begin{bmatrix} q_1(t) \\ q_2(t) \\ q_3(t) \end{bmatrix} = \hat{\mathbf{n}} \sin\left(\frac{\theta(t)}{2}\right) \tag{8}$$

and the scalar $q_4(t)$ is

$$q_4(t) = \cos\left(\frac{\theta(t)}{2}\right) \tag{9}$$

where $\hat{\mathbf{n}}$ is a unit vector indicating the principal rotation axis and θ is the principal rotation angle. The quaternion components satisfy the following normalization constraint:

$$\mathbf{q}^T\mathbf{q} = q_1^2 + q_2^2 + q_3^2 + q_4^2 = 1 \tag{10}$$

A three dimensional MRPs vector is defined as

$$\hat{\mathbf{a}}(t) \equiv \frac{4\mathbf{q}_{13}(t)}{1 + q_4(t)} \tag{11}$$

In the MEKF formulation, the true attitude quaternion $\mathbf{q}$ is represented by

$$\mathbf{q}(t) = \delta\mathbf{q}(\hat{\mathbf{a}}(t)) \otimes \mathbf{q}_{ref}(t) \tag{12}$$

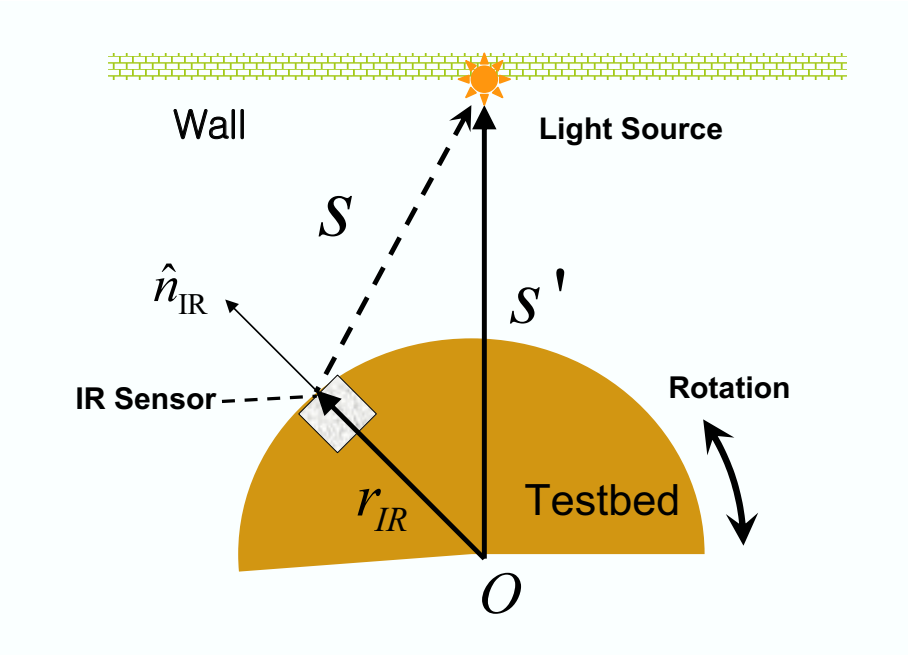

Figure 4. Testbed top view

where $\mathbf{q}_{ref}$ and $\delta\mathbf{q}(\hat{\mathbf{a}}(t))$ are the reference and the error quaternion in the body frame, respectively. The quaternion multiplication $\otimes$ is defined as[4]

$$\mathbf{q}' \otimes \mathbf{q} = \begin{bmatrix} q'_4\mathbf{q}_{13} + q_4\mathbf{q}'_{13} - \mathbf{q}'_{13} \times \mathbf{q}_{13} \\ q'_4 q_4 - \mathbf{q}'_{13} \cdot \mathbf{q}_{13} \end{bmatrix} \tag{13}$$

The error quaternion $\delta\mathbf{q}(\hat{\mathbf{a}}(t))$, which represents the error between the true and the reference attitude, can be expressed in terms of MRPs as[4]

$$\delta\mathbf{q}(\hat{\mathbf{a}}(t)) = \frac{1}{16 + a(t)^2} \begin{pmatrix} 8\hat{\mathbf{a}}(t) \\ 16 - a(t)^2 \end{pmatrix} \tag{14}$$

where a is the magnitude of the MRPs vector.

The quaternion kinematic equations of motion are given by

$$\dot{\mathbf{q}}(t) = \frac{1}{2} \begin{bmatrix} \boldsymbol{\omega}(t) \\ 0 \end{bmatrix} \otimes \mathbf{q}(t) \tag{15}$$

where $\boldsymbol{\omega}$ is the angular velocity of the body frame. In the MEKF, $\hat{\mathbf{a}}$ is chosen to keep $\hat{\mathbf{a}} \equiv \mathbf{0}$ during the state propagation so that the quaternion $\mathbf{q}_{ref}$ represents an estimate of correctly normalized true attitude estimate.

The gyroscope model is given by

$$\boldsymbol{\omega}(t) = \tilde{\boldsymbol{\omega}}(t) - \mathbf{b}(t) - \boldsymbol{\eta}_{\boldsymbol{v}}(t) \tag{16}$$

$$\dot{\mathbf{b}}(t) = \boldsymbol{\eta}_{\boldsymbol{\mu}}(t) \tag{17}$$

where $\tilde{\boldsymbol{\omega}}(t)$ represents the gyro output, $\mathbf{b}(\mathbf{t})$ is the gyro bias, $\boldsymbol{\eta}_{\boldsymbol{v}}(t)$ and $\boldsymbol{\eta}_{\boldsymbol{\mu}}(t)$ are uncorrelated zero-mean white noise processes.

The Kalman filter uses quaternion kinematics Eq. 15 with $\mathbf{q} = \mathbf{q}_{ref}$ and

$$\boldsymbol{\omega}(t) = \hat{\boldsymbol{\omega}}(t) = \tilde{\boldsymbol{\omega}}(t) - \hat{\mathbf{b}}(t) \tag{18}$$

$$\dot{\hat{\mathbf{b}}}(t) = \mathbf{0} \tag{19}$$

to propagate the filter state.

The error covariance propagation matrix $\mathcal{P}$ satisfies

$$\dot{\mathcal{P}}(t) = F\left[\hat{\mathbf{x}}(t), t\right]\mathcal{P}(t) + \mathcal{P}(t)F\left[\hat{\mathbf{x}}(t), t\right]^T + Q \tag{20}$$

where $F(t)$ and $G(t)$ matrices are given by

$$F(t) = \begin{bmatrix} -[\hat{\boldsymbol{\omega}}(t)\times] & -I_{3\times 3} \\ 0_{3\times 3} & 0_{3\times 3} \end{bmatrix} \tag{21}$$

$$G(t) = \begin{bmatrix} -I_{3\times 3} & 0_{3\times 3} \\ 0_{3\times 3} & I_{3\times 3} \end{bmatrix} \tag{22}$$

$$\tag{23}$$

and $Q(t)$ is the process noise covariance matrix of the following form

$$Q = \begin{bmatrix} \sigma_v^2 & 0 \\ 0 & \sigma_\mu^2 \end{bmatrix} \tag{24}$$

where the terms σ_v^2 and σ_μ^2 are the variances of η_v and η_μ, respectively.

The measurement update is done with the two vector measurements from the IR sensor and the inclinometers. The sensitivity matrix is given by

$$\mathbf{H} = \begin{bmatrix} \left[A(\mathbf{q})^N\hat{\mathbf{g}}\times\right] & \mathbf{0}_{3\times 3} \\ \left[A(\mathbf{q})^N\hat{\mathbf{s}}'\times\right] & \mathbf{0}_{3\times 3} \end{bmatrix}_{\mathbf{q}=\mathbf{q}_{ref}} \tag{25}$$

where A is the attitude matrix of the body frame with respect to an inertial frame. The vectors ${}^N\hat{\mathbf{g}}$ and ${}^N\hat{\mathbf{s}}'$ are the inertial frame representations of the vectors $\hat{\mathbf{g}}$ and $\hat{\mathbf{s}}'$.

Bad measurement data (large spikes), caused by disturbances from the testbed electrical components, are removed by monitoring the filter innovation vector residual before they are processed by the filter.

For further details on the MEKF, refer to Refs. 3, 4, and 6.

IV. Nonlinear Gyroscope Bias Observer

In this section, a nonlinear attitude and bias observer is derived based on Lyapunov's direct method. Like the MEKF, this observer estimates attitude and gyro bias by employing both the quaternion and the MRPs. It fully exploits the nonlinear structure of the attitude kinematics. As a consequence global convergence is guaranteed at least analytically, which means that the system can recover from large errors.

To design the nonlinear observer consider Eq. 12. The reference quaternion $\mathbf{q}_{ref}$ is defined such that it follows

$$\dot{\mathbf{q}}_{ref}(t) = \frac{1}{2}\begin{bmatrix} \boldsymbol{\omega}_{ref}(t) \\ 0 \end{bmatrix} \otimes \mathbf{q}_{ref}(t) \tag{26}$$

where the reference body rate is now defined as

$$\boldsymbol{\omega}_{ref}(t) \equiv \tilde{\boldsymbol{\omega}}(t) - \hat{\mathbf{b}}(t) - \boldsymbol{\epsilon}(t) \tag{27}$$

where $\boldsymbol{\epsilon}$ is a 3 by 1 vector, which will be defined later. The MRPs ($\hat{\mathbf{a}}$) satisfy the following kinematic equations:[4]

$$\dot{\hat{\mathbf{a}}} = [(1 - \frac{1}{16}a^2)I_{3x3} + \frac{1}{8}\hat{\mathbf{a}}\hat{\mathbf{a}}^T](\boldsymbol{\omega} - \boldsymbol{\omega}_{ref}) + \frac{1}{2}\hat{\mathbf{a}} \times (\boldsymbol{\omega} + \boldsymbol{\omega}_{ref}) \tag{28}$$

where $\boldsymbol{\omega}$ is the true body rate.

Consider the Lyapunov function candidate of the form

$$V(\hat{\mathbf{a}},\ \tilde{\mathbf{b}}) = \frac{1}{2}\alpha\hat{\mathbf{a}}^T\hat{\mathbf{a}} + \frac{1}{2}\beta\tilde{\mathbf{b}}^T\tilde{\mathbf{b}} \tag{29}$$

where α and β are positive constants, and the gyro bias estimate error $\tilde{\mathbf{b}} \equiv \hat{\mathbf{b}} - \mathbf{b}$. Then the time derivative of the Lyapunov function V is given by

$$\begin{aligned}\dot{V}(\hat{\mathbf{a}},\ \tilde{\mathbf{b}}) &= \alpha\hat{\mathbf{a}}^T\dot{\hat{\mathbf{a}}} + \beta\dot{\tilde{\mathbf{b}}}^{\mathbf{T}}\tilde{\mathbf{b}} \\ &= \alpha\hat{\mathbf{a}}^T[(1-\frac{1}{16}a^2)I_{3x3} + \frac{1}{8}\hat{\mathbf{a}}\hat{\mathbf{a}}^T](\boldsymbol{\omega}-\boldsymbol{\omega}_{ref}) + \beta\dot{\tilde{\mathbf{b}}}^{\mathbf{T}}\tilde{\mathbf{b}} \end{aligned} \tag{30}$$

where Eq. 28 is substituted and $\hat{\mathbf{a}}^T[\hat{\mathbf{a}} \times (\boldsymbol{\omega}+\boldsymbol{\omega}_{ref})] = \mathbf{0}$ is used. Using Eqs. 16 and 27, and neglecting the noise η_v, the vector $(\boldsymbol{\omega}-\boldsymbol{\omega}_{ref})$ in Eq. 30 can be expressed as $\boldsymbol{\omega}-\boldsymbol{\omega}_{ref} = \tilde{\mathbf{b}}+\boldsymbol{\epsilon}$. Then we can rewrite Eq. 30 as

$$\begin{aligned}\dot{V}(\hat{\mathbf{a}},\ \tilde{\mathbf{b}}) &= \alpha\hat{\mathbf{a}}^T[(1-\frac{1}{16}a^2)I_{3x3} + \frac{1}{8}\hat{\mathbf{a}}\hat{\mathbf{a}}^T](\tilde{\mathbf{b}}+\boldsymbol{\epsilon}) + \beta\dot{\tilde{\mathbf{b}}}^{\mathbf{T}}\tilde{\mathbf{b}} \\ &= \alpha[1+\frac{1}{16}a^2]\hat{\mathbf{a}}^T\tilde{\mathbf{b}} + \alpha[1+\frac{1}{16}a^2]\hat{\mathbf{a}}^T\boldsymbol{\epsilon} + \beta\dot{\tilde{\mathbf{b}}}^{\mathbf{T}}\tilde{\mathbf{b}} \end{aligned} \tag{31}$$

If we choose

$$\boldsymbol{\epsilon} = -\lambda\hat{\mathbf{a}} \tag{32}$$

$$\dot{\tilde{\mathbf{b}}} = -\frac{\alpha}{\beta}[1+\frac{1}{16}a^2]\hat{\mathbf{a}} \tag{33}$$

where λ is a positive constant, then $\dot{V}$ can be simply expressed as

$$\dot{V} = -\lambda\alpha[1+\frac{1}{16}a^2]a^2 \tag{34}$$

which is negative semi-definite.

Because $\dot{V} \leq 0$, the observer is only stable in the sense of Lyapunov but not asymptotically stable. To prove the asymptotic stability of the observer about $\hat{\mathbf{a}} = \mathbf{0}$ and $\tilde{\mathbf{b}} = \mathbf{0}$, we use theorem 8.5 of Ref. 8. According to the theorem, asymptotic stability can be achieved 1) if the first $k-1$ derivatives of $V(\mathbf{x})$ is zero when evaluated on the set $\boldsymbol{\Omega}$, which is the set of non-empty state vector satisfying $\mathbf{x} \in \boldsymbol{\Omega} \Longrightarrow \dot{V}(\mathbf{x}) = 0$, and 2) the k^{th} derivative of $V(\mathbf{x})$ is negative definite on the set $\boldsymbol{\Omega}$ with an odd number k.

Therefore the set $\boldsymbol{\Omega}$ can be calculated from Eq. 34 and is given by $\boldsymbol{\Omega} = \{(\hat{\mathbf{a}},\ \tilde{\mathbf{b}})|\hat{\mathbf{a}} = \mathbf{0}\}$. The second derivative of V is

$$\ddot{V} = -\lambda\alpha[2+\frac{1}{4}a^2]\hat{\mathbf{a}}^T[(1-\frac{1}{16}a^2)I_{3x3} + \frac{1}{8}\hat{\mathbf{a}}\hat{\mathbf{a}}^T](\tilde{\mathbf{b}}+\boldsymbol{\epsilon}) \tag{35}$$

which is still $\mathbf{0}$ when evaluated at $\boldsymbol{\Omega} = \{(\hat{\mathbf{a}},\ \tilde{\mathbf{b}})|\hat{\mathbf{a}} = \mathbf{0}\}$. Taking the time derivative of Eq. 35, the third derivative of V can be written as

$$\begin{aligned}\dddot{V} &= -\lambda\alpha\frac{1}{2}\hat{\mathbf{a}}^T\dot{\hat{\mathbf{a}}}\hat{\mathbf{a}}^T[(1-\frac{1}{16}a^2)I_{3x3} + \frac{1}{8}\hat{\mathbf{a}}\hat{\mathbf{a}}^T](\tilde{\mathbf{b}}+\boldsymbol{\epsilon}) - \lambda\alpha(2+\frac{1}{4}a^2)\dot{\hat{\mathbf{a}}}^T[(1-\frac{1}{16}a^2)I_{3x3} + \frac{1}{8}\hat{\mathbf{a}}\hat{\mathbf{a}}^T](\tilde{\mathbf{b}}+\boldsymbol{\epsilon}) \\ &- \lambda\alpha(2+\frac{1}{4}a^2)\hat{\mathbf{a}}^T(-\frac{1}{8}\hat{\mathbf{a}}^T\dot{\hat{\mathbf{a}}}I + \frac{1}{8}\dot{\hat{\mathbf{a}}}\hat{\mathbf{a}}^T + \frac{1}{8}\hat{\mathbf{a}}\dot{\hat{\mathbf{a}}}^T)(\tilde{\mathbf{b}}+\boldsymbol{\epsilon}) - \lambda\alpha[2+\frac{1}{4}a^2]\hat{\mathbf{a}}^T[(1-\frac{1}{16}a^2)I_{3x3} + \frac{1}{8}\hat{\mathbf{a}}\hat{\mathbf{a}}^T](\dot{\tilde{\mathbf{b}}}+\dot{\boldsymbol{\epsilon}}) \end{aligned} \tag{36}$$

Then evaluating Eq. 36 on the set $\boldsymbol{\Omega}$ and simplifying gives

$$-2\lambda\alpha(\tilde{\mathbf{b}}+\boldsymbol{\epsilon})^T(\tilde{\mathbf{b}}+\boldsymbol{\epsilon}) \tag{37}$$

which is negative definite for all $\boldsymbol{\Omega} = \{(\hat{\mathbf{a}},\ \tilde{\mathbf{b}})|\hat{\mathbf{a}} = \mathbf{0}\}$. Therefore we can conclude that Eqs. 28 and 33 are globally asymptotically stable with no noise. Assuming that the bias is nearly constant then $\dot{\tilde{\mathbf{b}}} \simeq \dot{\hat{\mathbf{b}}}$ can be used to estimate the bias with Eq. 33. Note that the attitude errors represented by MRPs can be obtained from Eq. 12 with the assumption that $\mathbf{q} \simeq \tilde{\mathbf{q}}$ where $\tilde{\mathbf{q}}$ is the quaternion measurement converted from the two vector observations. In this paper, we use the deterministic TRIAD algorithm[9] to determine an attitude from the gravity and the sun vector. In the TRIAD, the unit gravity vector is used as the first basis since it is more accurate then the sun vector which is from the IR sensor. Note that when noises are present in the measurements, estimated values still converge to the region around the true values within error-bounds which are related to the noise upper bounds.

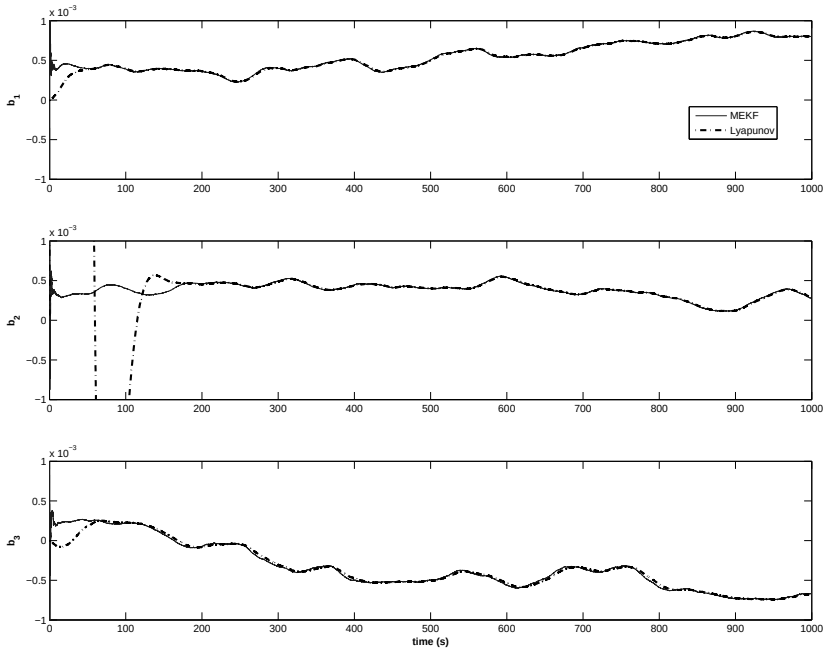

Figure 5. Bias estimate comparison

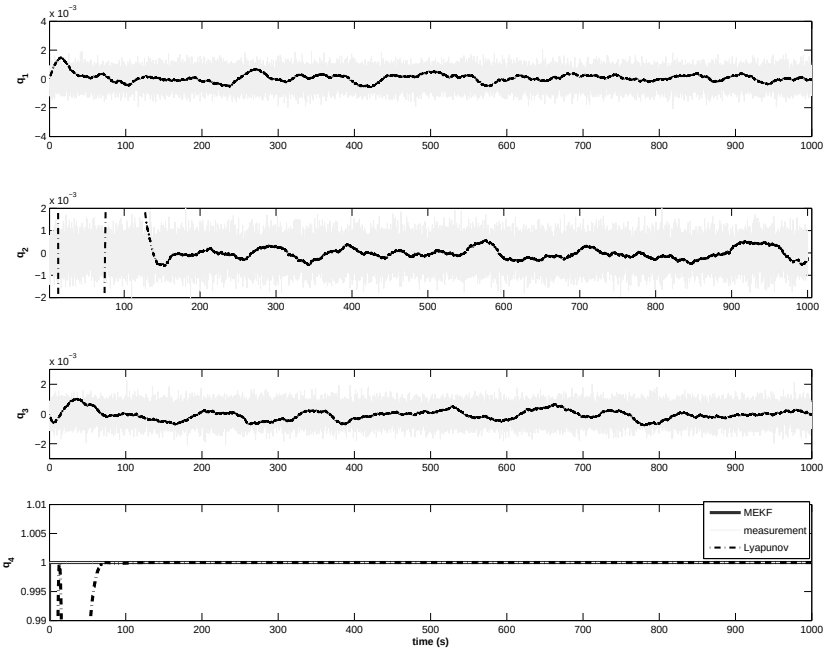

Figure 6. Attitude estimate comparison

V. Simulation and Experiment Results

In this section, several numerical simulations and experiments have been done to validate the MEKF and the Lyapunov observer in the presence of noise in the sensors data. The TASS has a Northrop Grumman Litton LN-200 IMU consisting of three fiber optics rate gyroscopes and a coarse two-axis analog sun sensor consisting of four photo-transistors.

A 20 W halogen source light is placed on the wall 3 m away from the TASS center of rotation. The gyro measurement data are simulated using Eqs. 16 and 17 with the noise standard deviations of $\sigma_{upsilon} = 0.0195^\circ/s^{1/2}$ and $\sigma_\mu = 0.0057^\circ/s^{3/2}$. Initial gyro bias of $\mathbf{b(t_0)} = [4.3\ 3.2\ 2.3]^T * 10^{-4}(rad/s)$ is used. For the simulations, a Gaussian white noise of $\sigma = 0.001$ has been added to the measurement of the gravity and the sun vector. The initial estimate for the attitude quaternion has been set to $\mathbf{q} = [0\ 0\ 1\ 0]^T$ (whereas the true attitude is $\mathbf{q} = [0\ 0\ 0\ 1]^T$) and the bias has been set to $\mathbf{b} = [0\ 0\ 0]^T$. Data sampling interval of 0.025 s has been chosen for all sensors with a 4th order Runge-Kutta method for the numerical integration method.

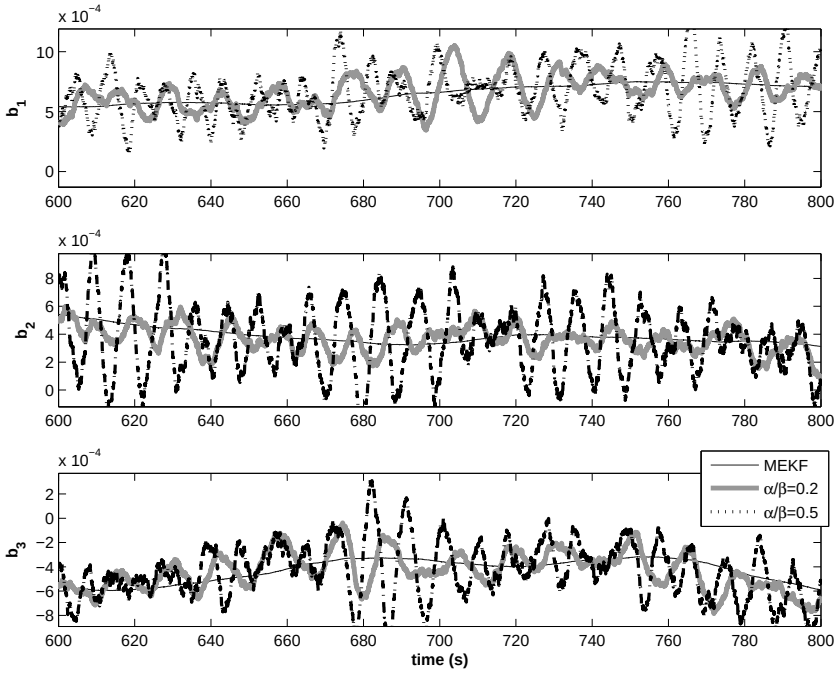

Figure 7. Effect of $\frac{\alpha}{\beta}$ changes on the Lyapunov observer estimate

Figures 5 and 6 show the comparisons of bias and attitude estimate computed using the MEKF and the nonlinear Lyapunov observer. For the Lyapunov observer, Λ and $\frac{\alpha}{\beta}$ of Eqs. 32 and 33 are chosen to be 0.1 and 0.005, respectively. We can see from the figures that the Lyapunov observer estimate accurately follows the estimate of the MEKF after 200 s.

The effects of changes in the values of $\frac{\alpha}{\beta}$ and λ on the estimation performance have been shown in Figs. 7 and 8, respectively. We can see from Fig. 7 that as $\frac{\alpha}{\beta}$ increases the bias estimate becomes more sensitive to the sensor noise. From Fig. 8, we can see that the value λ should be kept small to get a good performance in the presence of sensor noise.

For the experiments, standard deviations of the Gaussian white noises $\boldsymbol{\sigma} = [0.002\ 2 \times 10^{-6}\ 0.001]^T$ (gravity vector) and $\boldsymbol{\sigma} = [0.001\ 0.0099\ 0.0358]^T$ (sun vector) are used to tune the MEKF. Figure 9 shows the result of the bias estimate using both the MEKF and the Lyapunov observer. We can see from this figure that the estimated values for both algorithms are consistent.

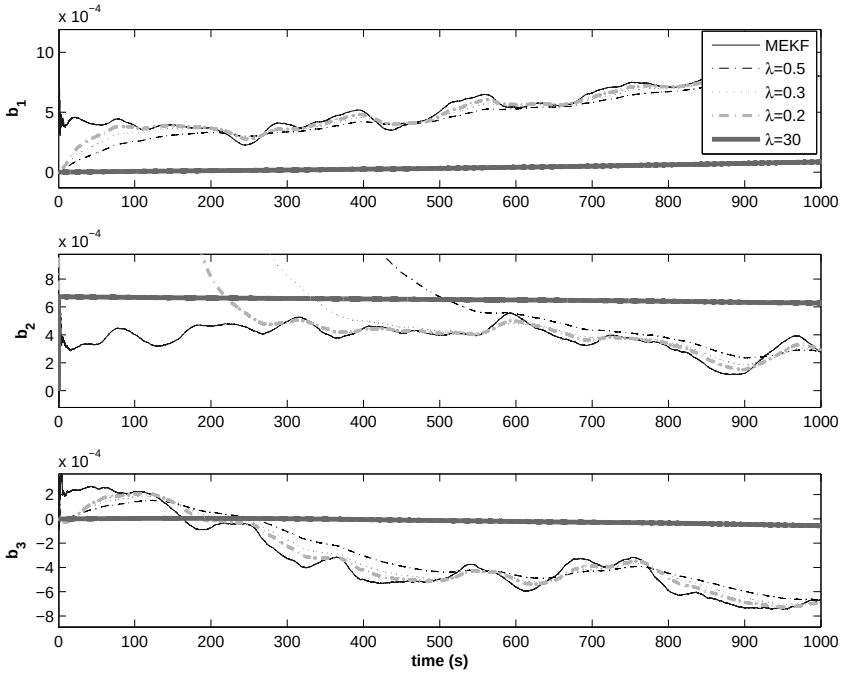

Figure 8. Effect of λ changes on the Lyapunov observer estimate

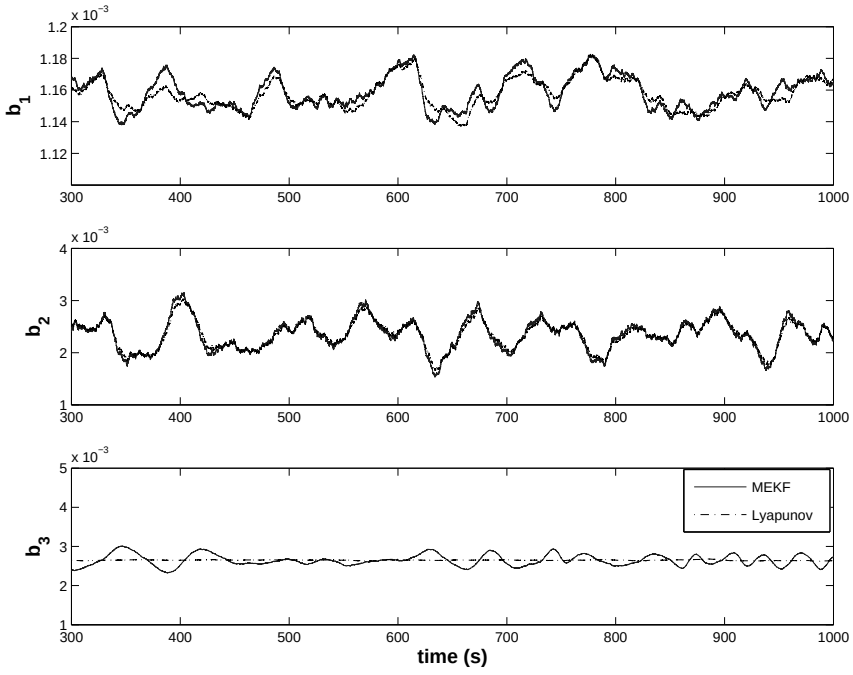

Figure 9. Actual bias estimate using the MEKF and the Lyapunov observer

VI. Conclusion

In this paper the attitude determination method for the NPS Bifocal Relay Mirror Spacecraft Simulator has been shown. The simulator simulates three-axis motion of the spacecraft. The nominal attitude determination approach is the MEKF based on the modified Rodrigues parameters (MRPs) as an unconstrained representation of the attitude error. The MEKF uses measurements from the two-axis analog IR sensor, two inclinometers, and gyroscopes. A method to extract the gravity vector from inclinometers has been shown with a compensation method for the effect of transitional motion of the IR sensor due to the rotation of the testbed. As an alternative for the MEKF method, a Lyapunov based nonlinear observer has been derived which provides a globally asymptotically stable algorithm. The nonlinear observer works well even in the presence of noises and large initial errors. In addition, it is easy to operate since we have only a few observer parameters to tune compared to the MEKF. Moreover the algorithm is very simple and computationally inexpensive. Numerical and experimental validations have been shown for both attitude determination algorithms. The main drawback of the nonlinear observer is that it needs high data sampling frequency.

Acknowledgments

The authors would like to acknowledge significant contributions in the development of these simulators by Guidance Dynamics Corporation, Automated Control Environments. This research was performed while Dr. Jong-Woo Kim held a National Research Council Research Associateship Award at the Naval Postgraduate School.

References

[1]Agrawal, B. N., "Acquisition, Tracking, and Pointing of Bifocal Relay Mirror Spacecraft," *American Astronautical Society*, Feb. 2003, AAS 03-151,.

[2]Agrawal, B. N., Romano, M., and Martinez, T., "Three axis Attitude Control Simulators for Bifocal Relay Mirror Spacecraft," *Advances in the Astronautical Sciences*, 2003, AAS 03-268,.

[3]Lefferts, E. J., Markley, F. L., and Shuster, M. D., "Kalman Filtering for Spacecraft Attitude Estimation," *Journal of Guidance, Control, and Dynamics*, Vol. 5, No. 5, Sept.-Oct. 1982, pp. 417–429.

[4]Markley, F. L., "Attitude Representations for Kalman Filtering," *Journal of Guidance, Control, and Dynamics*, Vol. 26, No. 2, March-April 2003, pp. 311–317.

[5]Crassidis, J. L. and Markley, F. L., "Unscented Filtering for Spacecraft Attitude Estimation," *Journal of Guidance, Control, and Dynamics*, Vol. 26, No. 4, July-August 2003, pp. 536–537.

[6]Crassidis, J. L. and Junkins, J. L., *Optimal Estimation of Dynamical Systems*, CRC Press, Boca Raton, FL, 2004.

[7]Seika.de, *N3 Product Description*, Jan. 2004, http://www.seika.de/english/Daten/N

[8]Schaub, H. and Junkins, J. L., *Analytical Mechanics of Space Systems*, AIAA Education Series, AIAA, Reston, VA, 2003.

[9]Wertz, J. S., editor, *Spacecraft Attitude Determination and Control*, D. Reidel Publishing Co., Dordrecht, The Netherlands, 1984.